

# Introducing Inkjet Printing Technology to the Fabrication of Flat-Layered Meta-Lens Antennas

Anastasios Papathanasopoulos and Yahya Rahmat-Samii  
Electrical and Computer Engineering Department  
University of California Los Angeles  
Los Angeles, CA, USA  
anastasispapath@g.ucla.edu,  
rahmat@ee.ucla.edu

Ryan Bahr, Yepu Cui, and Manos M. Tentzeris  
Electrical and Computer Engineering Department  
Georgia Institute of Technology  
Atlanta, GA, USA  
rbahr3@gatech.edu, yepu.cui@gatech.edu,  
etentze@ece.gatech.edu

**Abstract**—This paper presents for the first time the additive manufacturing using inkjet printing processes to construct flat-layered metamaterial lenses. In previous work, the metamaterial patterns on the lens layers were produced using an etching approach on commercially available dielectric copper-clad substrates. In this paper, the meta-lens consists of metamaterial square-rings that are inkjet-printed on ultra-thin dielectric layers of polyethylene terephthalate (PET) using silver nanoparticle ink. The metamaterial square-ring units of variable sizes are distributed on the thin dielectric layers to satisfy the required refractive index distribution. Simulation results of a 12 cm lens operating at 13.4 GHz demonstrate the collimating features of the proposed lens.

## I. INTRODUCTION

Flat-layered metamaterial lenses have been proposed as lightweight and thin alternatives to shaped homogeneous lenses [1], [2]. Flat-layered lenses consist of metamaterial metallic patterns on dielectric layers, where the size of the metamaterial elements varies to satisfy the required refractive index distribution [3]. The conventional method for the fabrication of flat-layered lenses is to use an etching approach on commercially available substrates, where the unneeded copper part is removed, as illustrated in Fig. 1. The disadvantages of this approach include: a) the choice of the commercially available copper-clad substrates is limited b) in etching, the waste includes hazardous chemicals, which are required to etch away the unwanted metal, and c) extra metal is used than necessary. To overcome these disadvantages, we propose for the first time the additive manufacturing using an inkjet printing process for the construction of flat-layered metamaterial lenses. Unlike the conventional etching methods, inkjet printing can be used on ultra-thin substrates that are not available with copper cladding. Inkjet printing is also a purely additive process, only depositing conductive lines where required, using as much ink as it needs, and producing no by-products [4]. In this paper, we present full-wave simulation results of a 12 cm-diameter inkjet printed lens operating at 13.4 and preliminary fabrication results of the lens layers.

## II. UNIT CELL

The lens unit cell consists of metamaterial square-rings on both sides of ultra-thin 125  $\mu\text{m}$ -thick dielectric substrates,

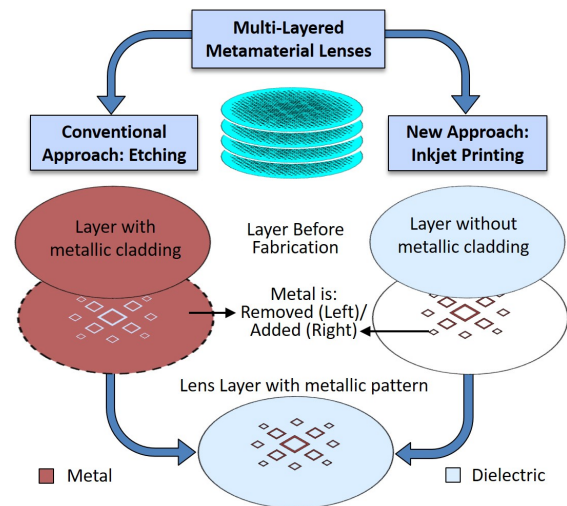


Fig. 1. High-level flowchart of the fabrication methods for the construction of flat-layered meta-lenses: i) etching approach and ii) additive manufacturing using inkjet printing.

as shown in Fig. 2. The unit cell is similar to the one that was used in [1] (the dielectric substrate is different here). The substrate used is polyethylene terephthalate (PET), a common thermoplastic polymer often used in disposable water bottles with  $\epsilon_r = 2.9$  and  $\tan \delta = 0.002$ . Note that the conventional etching approach cannot be applied to this substrate since it is not commercially available with copper cladding. The spacing foam material is the Rohacell 31HF with  $\epsilon_r = 1.046$  and  $\tan \delta = 0.0017$ . The unit cell was modelled in CST Microwave Studio using periodic boundary conditions and assuming normally incident plane waves with the results applicable to about 40 degrees off normal direction. The effective refractive index  $n$  can be calculated from the S parameters using the standard electromagnetic parameter retrieval method as in [1]. It can be observed from Fig. 2 that the refractive index can be tuned by changing the square ring size and a maximum value of 2.28 can be achieved.

## III. FABRICATION

The metamaterial elements are fabricated with additive manufacturing, using an inkjet printing process. The printer

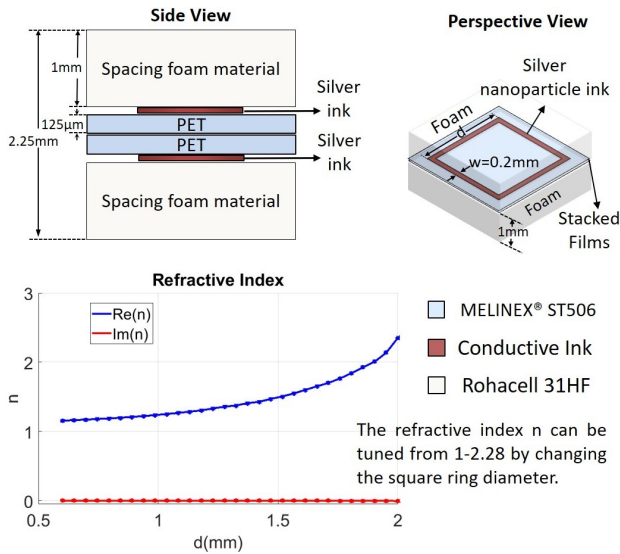


Fig. 2. Unit cell geometry and retrieved refractive index  $n$  as a function of the square ring size  $d$  at 13.4 GHz.

used is a Dimatix DMP-2800 series inkjet printer, with 16 nozzle cartridges with a drop spacing of  $20 \mu\text{m}$ , determining the pitch between the ink droplets. The conductive ink is based on silver nanoparticle (SunTronic EMD5730), which has a rated conductivity of at least  $5 \mu\Omega\cdot\text{cm}$ . The material has hydrophobic properties, which may cause liquids to bead on the surface, also considered the polymer's wettability. Before printing, the PET is exposed to a UV/O<sub>3</sub> process to improve the wetting of the ink on the substrate. This process improves how the droplet forms on the PET substrate, causing the ink to adhere immediately upon contact, improving the resolution of the printing process, as well as the adhesion and durability of the circuit design. In the current design, a single layer of silver nanoparticle ink is printed to improve the printing speed, with an estimated conductor thickness of  $0.5 \mu\text{m}$ . After printing, the PET is sintered for 30 minutes at the lowest temperature suggested for the ink, which is  $150^\circ\text{C}$ , to prevent deformation of the PET thermoplastic polymer. Fig. 3 shows photos of the printer as well as some representative quadrants of the fabricated layers.

#### IV. SIMULATION RESULTS

The lens diameter in this paper is  $D = 12 \text{ cm}$ , the multi-layered lens thickness is  $T = 3 \text{ cm}$ , the focal distance from the feed to the lens center is  $F = 7.3 \text{ cm}$ , the operating frequency is  $f = 13.4 \text{ GHz}$ , the maximum refractive index is 2.28 (which can be achieved using the metamaterial element in Fig. 2). The lens configuration and refractive index distribution are the same as in [1]. The lens is fed on axis, the feed is located at the origin and carries a  $\cos^{4.45}(\theta)$  amplitude pattern to taper the illumination to approximately -10 dB at the lens center. The unit cell of section II is used and the flat-layered lens is simulated using CST Microwave Studio. The results are shown in Fig. 4. It can be observed that the exit-aperture phase demonstrates uniformity and that the far-field radiation pattern is directional with a directivity of 23.3 dBi.

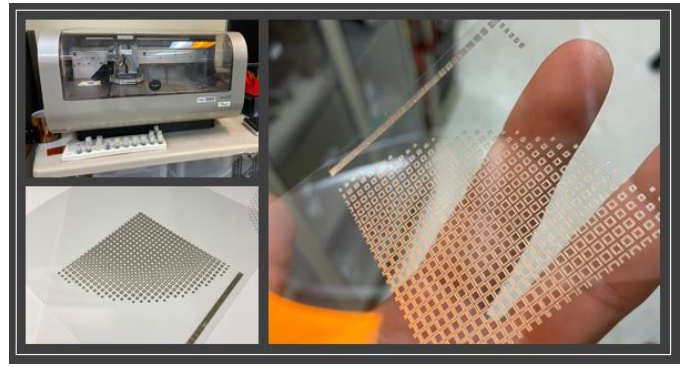


Fig. 3. Photo of the Dimatix DMP-2800 series inkjet printer and representative quadrants of the fabricated lens layers.

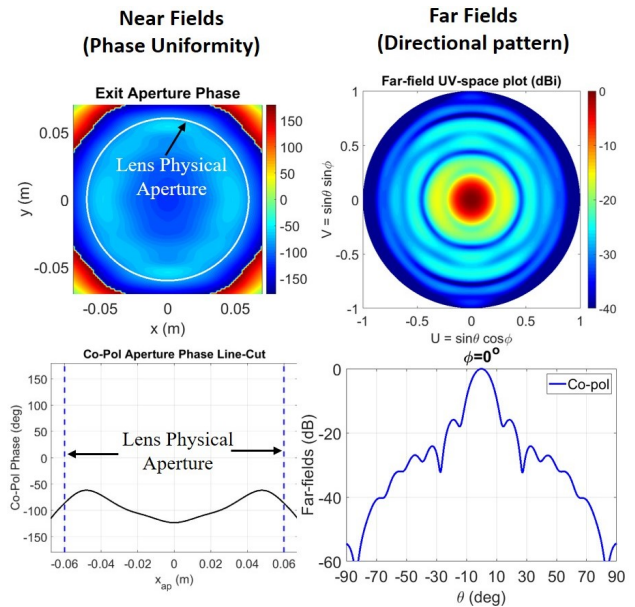


Fig. 4. Simulation results of the exit aperture near field phase distribution and the far field of the flat-layered 12 cm lens at 13.4 GHz. The simulated directivity is 23.3 dBi and the aperture efficiency is 76%.

#### ACKNOWLEDGEMENT

A. Papathanasopoulos' research was supported in part by grant 80NSSC19K1347 from NASA FINESST Program and Onassis Foundation-Scholarship ID: F ZP 042-1/2019-2020.

#### REFERENCES

- [1] A. Papathanasopoulos, Y. Rahmat-Samii, N. C. Garcia, and J. D. Chisum, "A novel collapsible flat-layered metamaterial gradient-refractive-index lens antenna," *IEEE Transactions on Antennas and Propagation*, vol. 68, no. 3, pp. 1312–1321, 2020.
- [2] A. Papathanasopoulos and Y. Rahmat-Samii, "Multi-layered flat metamaterial lenses: Design, prototyping and measurements," in *2020 Antenna Measurement Techniques Association Symposium (AMTA)*. IEEE, 2020.
- [3] —, "Flat meta-lens antenna synthesis via geometrical optics and particle swarm optimization," in *2020 IEEE International Symposium on Antennas and Propagation and CNC/USNC-URSI Radio Science Meeting*. IEEE, 2020, pp. 857–858.
- [4] S. Kim, B. Cook, T. Le, J. Cooper, H. Lee, V. Lakafosis, R. Vyas, R. Moro, M. Bozzi, A. Georgiadis, A. Collado, and M. M. Tentzeris, "Inkjet-printed antennas, sensors and circuits on paper substrate," *IET microwaves, antennas & propagation*, vol. 7, no. 10, pp. 858–868, 2013.